



# The extreme solar storm of May 1921: observations and a complex topological model

H. Lundstedt<sup>1</sup>, T. Persson<sup>2</sup>, and V. Andersson<sup>1</sup>

<sup>1</sup>Swedish Institute of Space Physics (IRF), Lund, Sweden

<sup>2</sup>Centre for Mathematical Sciences, Lund University, Lund, Sweden

Correspondence to: H. Lundstedt (henrik@lund.irf.se)

Received: 4 June 2014 – Revised: 19 November 2014 – Accepted: 29 December 2014 – Published: 27 January 2015

**Abstract.** A complex solid torus model was developed in order to be able to study an extreme solar storm, the so-called “Great Storm” or “New York Railroad Storm” of May 1921, when neither high spatial and time resolution magnetic field measurements, solar flare nor coronal mass ejection observations were available. We suggest that a topological change happened in connection with the occurrence of the extreme solar storm. The solar storm caused one of the most severe space weather effects ever.

**Keywords.** Solar physics astrophysics and astronomy (magnetic fields)

## 1 Introduction

Today’s high-tech society has become very vulnerable to strong solar storms, such as coronal mass ejections (CMEs) and solar flares. Fast Earth-directed CMEs may cause severe geomagnetic storms with large  $dB/dt$  variations and accompanied problems for the power industry (Lundstedt, 2006). Intense solar flares may cause problems for HF communications and aviation. Sixteen regional warning centres (RWCs) within the International Space Environment Service (ISES) provide world-wide forecast services of solar storms and space weather effects. RWC-Sweden (Swedish Space Weather Center) is operated by the Swedish Institute of Space Physics (IRF), in Lund. We offer warnings and forecasts based on space- and ground-based observations. Agencies around the world, among them the Swedish Civil Contingencies Agency (MSB), now work together in order to prepare for severe space weather effects. However, the latest research and observations show that we lack the necessary knowledge to understand and warn for extreme solar storms

and possible severe geoeffects. Historical records and astronomical observations of solar-type stars also tell us that we may be exposed to much stronger solar storms in the future. Flares up to a thousand times stronger have been observed on a solar-like star (Maehara et al., 2012). It is important to have warning of severe/extreme solar storms several days ahead, far enough in advance to be able to take action. Recent studies of extreme solar storms (Cannon, 2013) suggest that they occur much more often than just every 150 years and also that they can occur at any time during the sunspot cycle, i.e. not just close to solar maximum; they can occur even during weak sunspot cycles such as the present solar cycle 24. The most famous extreme solar storm, in September 1859, occurred during a weak cycle. This event, the so-called Carrington event, is often used as a measure of the most extreme solar storm and has been called a super solar storm. However, at that time solar magnetic fields were not measured, making it difficult to classify as an extreme solar storm (Lundstedt, 2010, 2012). In 1908 George Hale at Mount Wilson (MW) Observatory was able to measure the solar magnetic field using the Zeeman effect, a breakthrough in the search for a pattern behind solar activity and solar storms. In this paper we describe an attempt to use changes of the magnetic complexity to understand the extreme solar storm of May 1921, the first extreme event for which solar magnetic field measurements are available.

## 2 Solar observations

The active region (AR), with Mount Wilson number 1842, of May 1921 was observed for the first time on 8 May on the east limb at  $85^\circ$ . Since it was already large on 8 May, it must have evolved on the far side of the Sun. It was followed

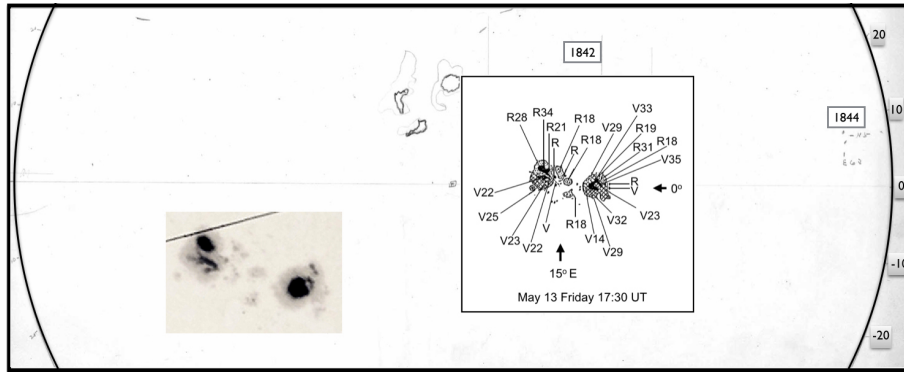


**Figure 1.** Mount Wilson drawing of active regions occurring on 13 May 1921 at 17:30 UT and to the left, a white-light observation by Royal Greenwich Observatory (RGO) at 09:55 UT.

up until 19 May at  $61^\circ$  on the west limb. Only the group following the Hale polarity law survived to the next rotation and appeared at the centre of the Sun on 10 June (Tamm, 1922). As can be seen in Fig. 1, only one small active region (AR 1844) appeared at the same time. Whether connected activity took place on the Earth-facing side of the Sun or not is hard to tell since the observer focused on AR 1842 (Title, 2012).

The active region 1842 in 12–16 May 1921 (RGO, 1955; Silverman and Cliver, 2001; Tamm, 1922) showed magnetic complexity ( $\beta$ - $\gamma$ ) and was located between  $26^\circ$  E and  $27^\circ$  W longitude at low latitude (Fig. 2). The spot group, Greenwich number 9334, had a large mean area of 1324 millionths of the Sun's visible hemisphere. The region 9334 with three large sunspots showed large flux changes especially on 12 May, but fluxes also disappeared and new fluxes emerged on 13 and 14 May 1921. The observer Eddison Petit at Mount Wilson made a note on the drawing that both H-alpha and K lines were bright, i.e. we also had strong solar flares on 12 May. We also notice a rotation of both sunspot groups, from having a line of polarity separation parallel to the equator to one perpendicular to it. When the large region after 12 May was broken up into two regions, the left started to rotate counter clockwise and the right clockwise. New negative flux was also seen to emerge on 14 May. Mount Wilson measured very strong magnetic flux densities of between  $+0.34$  and  $-0.35$  T (Fig. 2). These values have been corrected (Livingston et al., 2006) to  $+0.35$  and  $-0.36$  T. We notice that reduction of magnetic complexity took place at the times of the solar storms. Interestingly, Schrijver (2009) suggests in his review that the emergence of twisted flux ropes into pre-existing strong field plays a critical role for many, if not all, of the active regions that produce M- or X-class flares. As for the Carrington event, the solar storms 9334 in 1921 occurred during a moderate sunspot cycle and during the declining phase of cycle 15.

### 3 Terrestrial effects

Geomagnetic storm activity occurred mainly at about 20:00 UT on 13 May (Royal Greenwich Observatory, 1955), at 21:00–24:00 UT on 14 May and at 04:00–06:00 UT on 15 May (Silverman and Cliver, 2001). A sudden commencement (S.C.) and arrival of the first CME occurred at 13:10 UT on 13 May (Royal Greenwich Observatory, 1955). The next S.C. occurred at 22:20 UT on 14 May (Silverman and Cliver, 2001) and signalled the arrival of a new CME. The first CME may have cleared the way for the second one in the same way as occurred in an extreme solar storm on 23 July 2012 (Baker et al., 2013). Interestingly, a value for the rate of change of the horizontal component of the geomagnetic field  $dB_h/dt$  as high as about  $5000 \text{ nT min}^{-1}$  has been estimated for 14–15 May in Sweden (Kappenman, 2006). At 00:00 UT (02:00 local time) in the morning of 15 May a fire occurred in a telegraph station in Karlstad, Sweden (Em, 1921). Aurora was observed as close to the magnetic equator as Samoa (Silverman and Cliver, 2001), making the 1921 event one of the strongest space weather events ever reported.

### 4 Complex topological models

In order to be able to study an extreme solar storm, such as the one in May 1921, i.e. before high spatial and time-resolved vector magnetic field measurements and velocity measurements existed, we developed a complex torus model. The complexity is mathematically produced by an iterative mapping of a torus of magnetic flux tubes (Fig. 3).

A complex solid torus (Devaney, 2003) model was developed in order to address three questions:

1. Can parameters describing the complexity be extracted using a solid torus model from a picture of magnetic flux distribution or magnetogram?

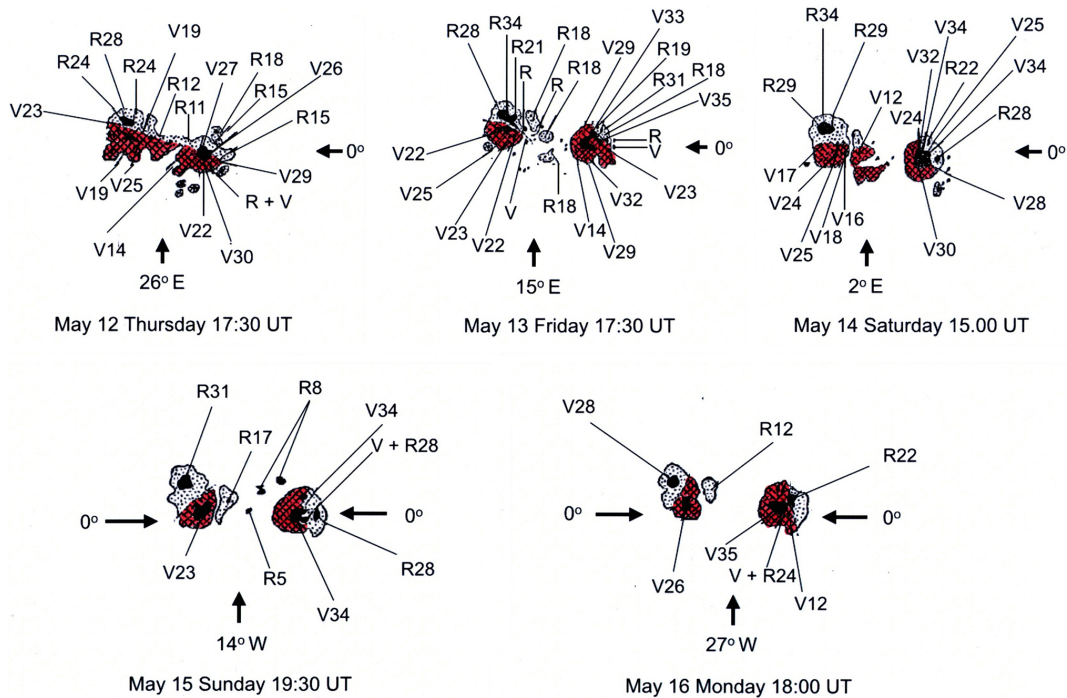


**Figure 2.** Active region 1842 observed at the Mount Wilson Observatory between 12 and 16 May 1921. V stands for negative magnetic field and R for positive. V25 e.g. corresponds to  $-0.25$  T or corrected  $-0.24$  T (Livingston et al., 2006). Large hatched areas of negative polarity are coloured red. When the large region after 12 May is broken up into two regions, the left starts to rotate counter-clockwise and the right clockwise. New negative flux is also seen to emerge on 14 May.

2. Can the solid torus model be used to reconstruct magnetograms and also make a study of the evolution of the active regions?
3. Can a probable explanation be found of the extreme solar storm of May 1921?

Let us start with the first question.

#### 4.1 A complex solid torus model of magnetograms and information extraction

We can parameterize the torus  $\mathbb{T}$  with the coordinates  $(\theta, z)$  where  $0 \leq \theta < 2\pi$  and  $z \in \mathbb{C}$ ,  $|z| \leq 1$ . Let  $a$  be an integer,  $a \geq 1$ ,  $b \in \mathbb{C}$ ,  $|b| < 1$ ,  $c \in \mathbb{C}$ , and  $d$  an integer,  $d \geq 1$  (unless  $a = 1$  in which case  $d \geq 0$ ) and  $\text{gcd}(a, d) = 1$  (Fig. 3 to the left).

Consider the map (Katok and Hasselblatt, 2006)

$$F : (\theta, z) \mapsto (a\theta, bz + ce^{id\theta}). \quad (1)$$

Hence  $F$  maps the torus into a torus that has been “folded”  $a$  times.

We assume that  $b$  and  $c$  are chosen so that  $F$  maps the torus into itself. Consider the set  $F(\mathbb{T})$  at the section  $\theta = \theta_0$ . The parameter  $a$  is the number of connected components of  $F(\mathbb{T})$ .

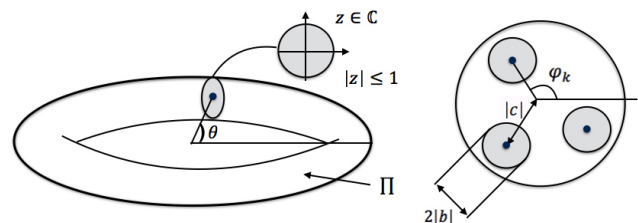


**Figure 3.** A torus  $\mathbb{T}$  is parameterized with the coordinates  $(\theta, z)$  to the left and a mapped cross-section is shown to the right.

The preimages of the points in  $F(\mathbb{T})$  at the section  $\theta = \theta_0$  are the points with

$$\theta = \frac{\theta_0}{a} + \frac{2\pi}{a}k, \quad k = 0, 1, \dots, a - 1. \quad (2)$$

Hence, the section of  $F(\mathbb{T})$  at  $\theta = \theta_0$  is the set

$$\{bz + ce^{id(\theta_0/a + 2\pi k/a)} : |z| < 1, k = 0, 1, \dots, a - 1\}. \quad (3)$$

We can therefore get some information about the parameters according to the picture to the right in Fig. 3. For  $k = 0, 1, \dots, a - 1$  we have

$$\phi_k = \gamma + d\left(\frac{\theta_0}{a} + \frac{2\pi}{a}k\right), \quad (4)$$

where  $\phi_k$  is defined in Fig. 3 and  $\gamma$  is such that  $c = |c|e^{i\gamma}$ .

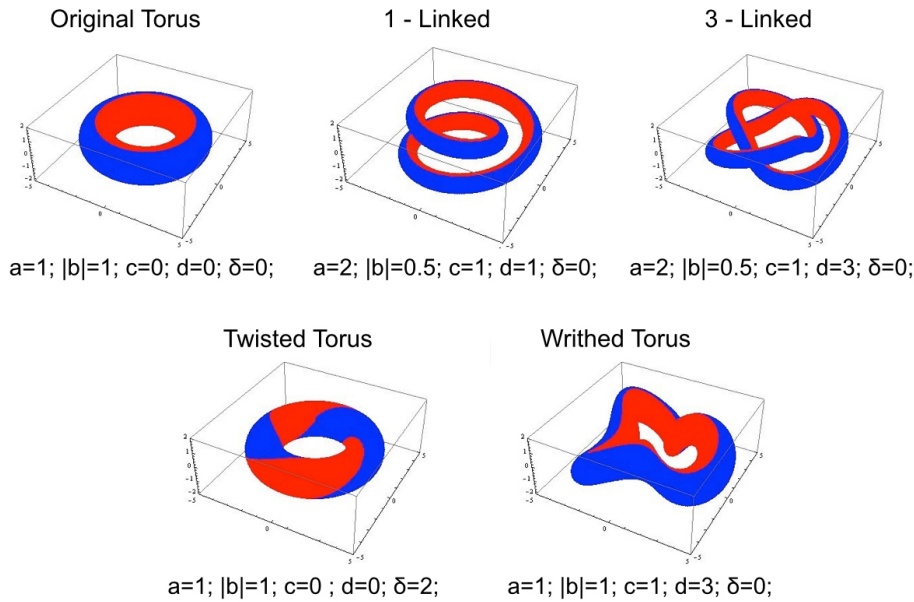


**Figure 4.** The first solid torus to the left shows the original torus. By changing the parameter  $d$  to 1 or 3 we obtain a one- or a three-linked torus. By changing  $\delta$  from 0 to 2 for the original torus we obtain a twisted torus. Finally by changing the  $c$  to 1 and  $d$  to 3 for the original torus we obtain a writhed torus.

We have now seen that we can extract complexity parameters from a picture.

Let us now address the second question and try to reproduce magnetograms from different values of these complexity values for the torus.

#### 4.2 Reconstruction of magnetograms using the torus model

With  $b = |b|e^{i\delta}$  we can write the map  $F$  as

$$F(\theta, z) = (a\theta, |b|e^{i\delta}z + |c|e^{i\gamma+id\theta}). \tag{5}$$

By changing the values of  $a, b, c, d$  and the angle  $\theta$  we can describe by  $F^n(\mathbb{T})$ , where the number of iterations  $n$  is a positive integer, a linked, a twisted and writhed solid torus. The parameter  $a$  describes how many times the curve winds about the centre,  $|b|$  changes the thickness of the image of the solid torus,  $|c|$  determines the separation of the solid torus parts in the cross-sectional planes,  $(a - 1)d$  is the linking number of the image of the solid torus and finally the parameter  $\delta$  determines the twist of the torus. The solid torus is then cut along its circular axis in two parts. These are the blue and red parts shown in Fig. 4. The two parts will be treated as positive and negative poles.

In Fig. 4 we give a couple of examples. The first solid torus to the left shows the original torus. By changing the parameter  $d$  to 1 or 3 we obtain a one- or a three-linked torus. By changing  $\delta$  from 0 to 2 for the original torus we obtain a twisted torus. Finally by changing the  $c$  to 1 and  $d$  to 3 for the original torus we obtain a writhed torus.

We cut the torus at an angle  $\theta$  and then calculate a simulated magnetogram from this cut as follows: for each point  $y$  in the simulated magnetogram, the intensity is given by the integral

$$\int \rho(x)|y - x|^{-2} dV(x),$$

where the integral is over all point  $x$  in the cut, and  $dV$  denotes the area measure. The function  $\rho(x)$  is defined to be 0 if  $x$  is outside the torus, and  $\rho(x) = \pm 1$  depending on which part of the torus  $x$  is in. In the computer, this integral is approximated by a finite sum.

We can also simulate magnetograms at any time in between. The colour code has been chosen to be the same as for observed HMI, SDO magnetograms. The most simple simulated magnetogram is obtained by taking a cut of the original torus into two adjacent tori with halved cross-sectional area (treated as positive and negative poles) and a grid of values is calculated based on their inverse distance squared. We may then e.g. map the torus once ( $n = 1$ ), and take cuts at  $\theta = 120^\circ$  or  $\theta = 360^\circ$  and obtain the other magnetograms (Fig. 5).

The solenoid is an attractor which is contained in a “solid torus” (Devaney, 2003). We would therefore expect iterating  $F$  should produce fractal magnetograms.

The magnetograms in Fig. 6 show exactly that.

Before trying to reproduce the magnetograms of May in 1921 we give two examples of more recent magnetograms observed by HMI on SDO (Fig. 7). As can be seen we capture the general structure, but a more fractal structure should have been included. For more complicated regions we also need

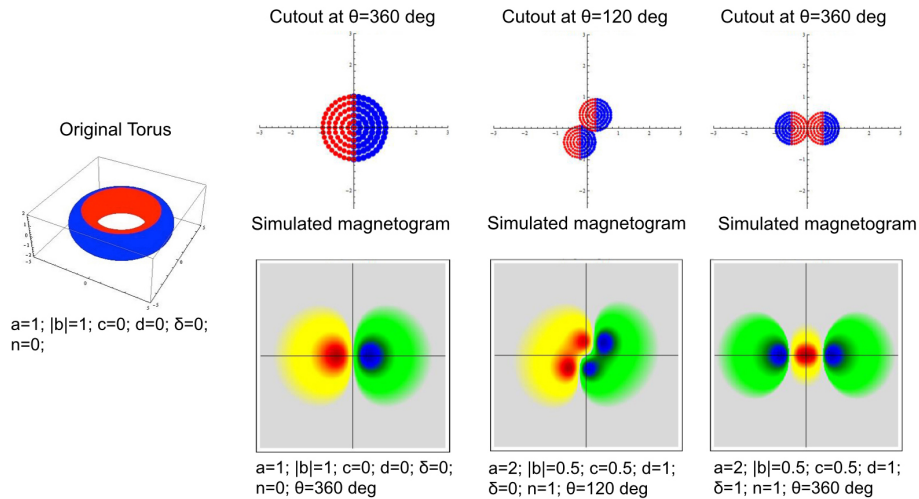


**Figure 5.** The most simple simulated magnetogram is obtained by taking a cut of the original torus into two equal semicircles (treated as positive and negative poles) and a grid of values is calculated based on their inverse distance squared to the semicircles. We may then e.g. map the torus once ( $n = 1$ ), and take cuts at  $\theta = 120^\circ$  or  $\theta = 360^\circ$  and obtain the other magnetograms.

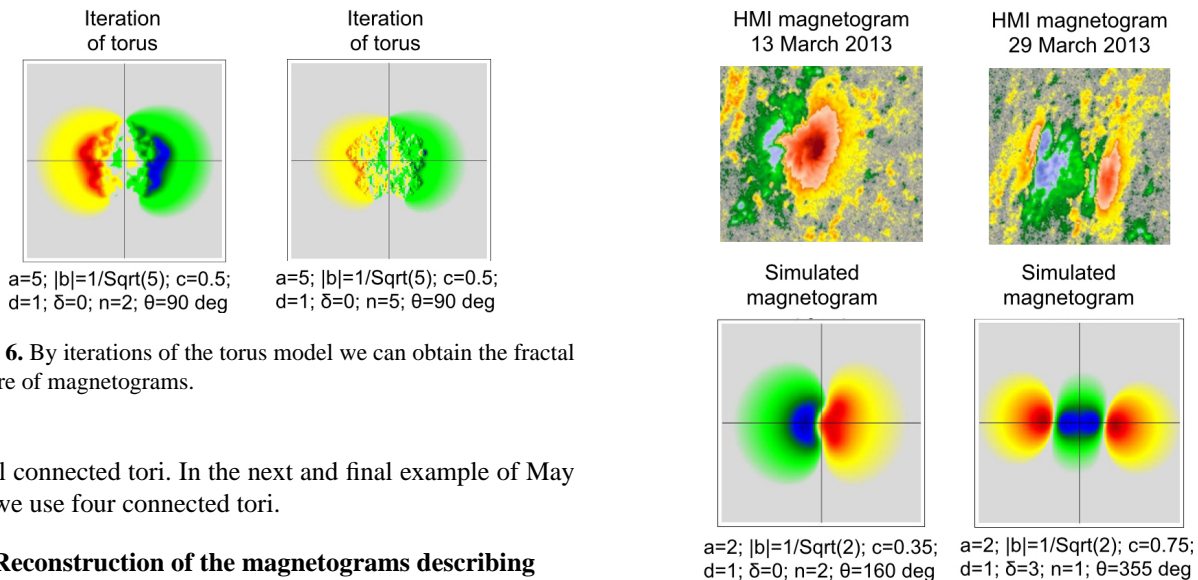


**Figure 6.** By iterations of the torus model we can obtain the fractal structure of magnetograms.

several connected tori. In the next and final example of May 1921 we use four connected tori.

### 4.3 Reconstruction of the magnetograms describing the extreme solar storm of 1921

Finally, we address the third question. We will reproduce the magnetograms of May 1921 and then try to understand what caused the extreme solar storm and when it occurred.

We use four tori to reproduce the magnetograms for 12 to 16 May (Fig. 8). It is assumed that these four tori are connected. The parameter sets used are displayed in Table 1.

We start with 12 May at 18:00 UT and after the break-up into two major regions which seems to have taken place on 13 May UT morning. We then try to reproduce the changes in the magnetograms topologically, i.e. by continuous change of  $\theta$  and  $z$ . On 13 May the left region starts to rotate anticlockwise to follow the Hale law. The right region starts to rotate clockwise. On late 13 to early 14 May we notice both emerging of flux and large rotations especially for the active re-

**Figure 7.** Two HMI magnetograms observed by SDO on 13 and 29 March 2013. Below are the parameters to give a solid torus model that can simulate the magnetograms.

gion right-hand side. A dramatic change seems to take place. We were unable to reproduce the observed magnetograms by continuous changes of  $\theta$  and  $z$ , but had to rotate the simulated magnetogram. We therefore find it probable that this rotation, caused by the opposite rotation of the two main pairs of opposite polarity, produced a topological change and that reconnection had taken place which would have explained the energy release and thus the extreme solar storm of 14 May. The CME then reached Earth at about 22:00 UT on 14 May.

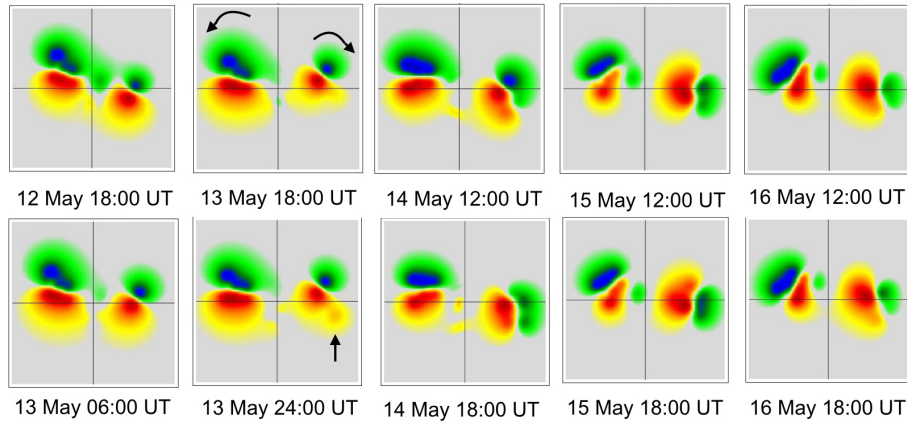


**Figure 8.** Simulated magnetograms from 12–16 May 1921. On 13 May the active regions start to rotate and new flux emerges.

**Table 1.** The set of parameters of the four tori used to simulate the magnetogram of 12 May 1921.

Parameters	12 May 1921			
$a$	2	2	3	1
$b$	$\frac{1}{\sqrt{2}}$	$\frac{1}{\sqrt{2}}$	$\frac{1}{\sqrt{3}}$	1
$c$	0.4	0.1	0.5	0.5
$d$	1	1	3	0
$\delta$	0	3	-3	1
$n$	2	1	1	1
$\theta$	284	360	294	150

#### 4.4 Further research

There are many possible extensions of the solid torus approach. A natural extension is to start trying to reconstruct magnetograms of higher time and spatial resolution, such as the magnetograms produced by HMI onboard SDO (Hoeksema et al., 2014), something we have already prepared for. With measurements of vector magnetic fields we will be able to make estimation of the energy release and give a better description of the magnetic complexity.

It would be very interesting to try to estimate the energy released during the extreme solar storm based on the change of the complexity parameters of the torus. Berger (1993) estimated that the free energy  $E_m$ , stored in the braided field, is proportional to the square of the crossing number  $C_{\min}$ :

$$E_m \geq 9.06 \times 10^{-2} C_{\min}^2 \frac{\Phi^2}{N^2 L}, \quad (6)$$

where  $\Phi$  is the magnetic flux of the flux tubes,  $N$  the number of strands of the braid (= flux tubes) and  $L$  the length. The linking numbers are closely related to the average crossing number, which is an algebraic measure of the link complexity in space (Ricca, 2002). Interestingly it is also found (Berger and Asgari-Targhi, 2009) that the energy released due to re-

connection of the braids in the coronal loops follows a power-law distribution, i.e. is fractal.

We have used several solid tori to describe large complex active regions and the evolution. It would also be interesting to study the small–large-scale magnetic field coupling as seen at times of solar flares and the Hale Solar Sector Boundary (Svalgaard et al., 2011; Lundstedt et al., 1980).

How quickly might a severe solar storm develop into an extreme storm? With an estimate of the energy release based on the parameters of the torus, this would be an interesting issue to examine. In the case of the 1921 event it took less than a week. During the Halloween events in 2003 (Weaver et al., 2004) it also took less than a week between the severe solar storms of 28 and 29 October and the extreme solar storm of 4 November. During the most recent event in July 2012 it took more than a week when the active region was on the far side (Lui et al., 2014). The solar storms of AR 11 520 in July 2012 reached a  $\beta$ – $\gamma$ – $\delta$ . For that occasion we can also use the parameters describing the complexity based on SDO observations and available complexity parameters through Space weather Helioseismic and Magnetic Imager Active Region Patches (SHARP) (Bobra et al., 2014), something which will be further discussed in an upcoming paper. The region grew to a size of 1460 millionths, an intrusion of negative polarity flux occurred in the positive umbra of the spot on 12 July at 13:00 UT and disappeared on 14 July at 09:00 UT. It produced an X 1.4 solar flare. A halo CME also occurred producing a proton event of about 100 pfu. An interesting coronal S-shaped sigmoid structure occurred just before the onset of the solar flare. One may therefore suspect that a kink instability occurred (Török et al., 2010). Not until it was on the far side did the active region 11 520 become an extreme solar storm. On 23 July it produced a very fast CME of  $3400 \text{ km s}^{-1}$  (Baker et al., 2013). We therefore expect that an extreme solar storm occurred on the far side of the Sun. Based on observations by STEREO of the velocity and magnetic field, a model was used to calculate a hypothetical  $\text{dB}/\text{dt}$  if the CME was headed toward Earth. A value

somewhat larger than  $1000 \text{ nT min}^{-1}$  was found, making it a candidate for an extreme solar storm. The geomagnetic storm index for the 2012 event was estimated as  $-1154 \text{ nT}$ , larger than that of the Carrington event at  $-850 \text{ nT}$  (Lui et al., 2014).

Finally, a follow-up of the work in Lundstedt and Persson (2010) would be to examine whether or not the seeming lack of coupling between the intensity of the extreme solar storms and intensity of the cycle has been the case only for recent cycles.

## 5 Summary

Magnetic field measurements carried out at the Mount Wilson Observatory as long ago as 1908 have made it possible for us to interpret the extreme solar storm in May 1921 based on the change and complexity of the magnetic field. In this paper we describe an attempt based on a complex solid torus model. A topological change is suggested at the time of the extreme solar storm. The model also makes it possible to study the development of an active region. The model will be further developed in order to even make use of today's magnetic field measurements by HMI onboard SDO (Hoeksema et al., 2014). The use of the SHARP service (Bobra et al., 2014) would make it operational. Being able to warn when a severe solar storm will develop into an extreme one is of great importance in order to be able to mitigate the effects for society.

*Acknowledgements.* We thank Todd Hoeksema and the SDO HMI solar team at Stanford, the SDO AIA team at Lockheed, the SOHO team, the Mount Wilson Observatory, Sarah Matthews, Univ. College London, Dept. of Space & Climate Phys. Solar & Stellar Physics Group, Mullard Space Science Laboratory for RGO 1921 for the data used, and geomagnetic field data for  $dB/dt$  estimations from World Data Centre Geomagnetism, British Geological Survey (BGS), Edinburgh, Instituto Nazionale di Astrofisica (INAF), Catania, Italy and NOAA Space Weather Prediction Center, USA. Finally we thank two referees, Mauro Messerotti and one anonymous, for helping to improve the paper.

Topical Editor M. Temmer thanks M. Messerotti and one anonymous referee for their help in evaluating this paper.

## References

Baker, D. N., Li, X., Pulkkinen, A., Ngwira, C. M., Mays, M. L., Galvin, A. B., and Simunac, K. D. C.: A major solar eruptive event in July 2012: Defining extreme space weather scenarios, *Space Weather*, 11, 585–591, 2013.

Berger, M.: Energy-Crossing Number Relations for Braided Magnetic Fields, *Phys. Rev. Lett.*, 70, 705–708, 1993.

Berger, M. A. and Asgari-Targhi, M.: Self-organized braiding and the structure of coronal loops, *Astrophys. J.*, 705, 347–355, 2009.

Bobra, M. G., Sun, X., Hoeksema, J. T., Turmon, M., Liu, Y., Hayashi, K., Barnes, G., and Leka, K. D.: The Helioseismic and Magnetic Imager (HMI) Vector Magnetic Field Pipeline: SHARPs – Space weather HMI Active Region Patches, *Sol. Phys.*, 289, 3549–3578, doi:10.1007/s11207-014-0529-3, 2014.

Cannon, P.: Extreme space weather: impact on engineered system and infrastructure, Royal Academy of Engineering, UK, 2013.

Devaney, R. L.: An Introduction to Chaotic Dynamical Systems, Second Edition Westview Press, Advanced Book Program, 2003.

Em, A. A.: Jordströmmar såsom brandstiftare, *Brandskydd*, 77–79, 1921 (in Swedish).

Hoeksema, J. T., Lui, Y., Hayashi, K., Sun, X., Schou, J., Couvidat, S., Norton, A., Bobra, M., Centano, R., Leka, K. D., Barnes, G., and Turmon, M.: The Helioseismic and Magnetic Imager (HMI) Vector Magnetic Field Pipeline: Overview and Performance, *Sol. Phys.*, 289, 3483–3530, doi:10.1007/s11207-014-0516-8, 2014.

Kappenman, J. G.: Great geomagnetic storms and extreme impulsive geomagnetic disturbance events – An analysis of observational evidence including the great storms of May 1921, *Adv. Space Res.*, 38, 188–199, 2006.

Katok, A. and Hasselblatt, B.: Introduction to the modern theory of dynamical systems, *Encyclopedia of Mathematics and its Applications*, edited by: Rota, G.-C., Vol. 54, Cambridge, 2006.

Livingston, W., Harvey, J. W., and Malanushenko, O. V.: Sunspots with the strongest magnetic fields, *Sol. Phys.*, 239, 41–68, 2006.

Lui, Y. D., Luhmann, J. G., Kajdic, P., Kilpua, E., Lugaz, N., Nitta, N. V., Möstl, C., Lavraud, B., Bale, S. D., Farrugia, C. J., and Galvin, A. B.: Observations of an Extreme Storm in Interplanetary Space Caused by Successive Coronal Mass Ejections, *Nature Communications*, 5, 3481, 2014.

Lundstedt, H.: The Sun, space weather and GIC effects in Sweden, *Adv. Space Res.*, 37, 1182–1191, 2006.

Lundstedt, H.: Solar storms, cycles and topology, *Eur. Phys. J.*, 9, 95–103, 2010.

Lundstedt, H.: Solar storms and topology: Observed with SDO, in: *Proceedings of TIEMS conference “Space Weather and Challenges for Modern Society”*, 22–24 October 2012.

Lundstedt, H. and Persson, T.: Modelling solar cycle length based on Poincaré maps for Lorenz-type equations, *Ann. Geophys.*, 28, 993–1002, doi:10.5194/angeo-28-993-2010, 2010.

Lundstedt, H., Wilcox, J. M., and Scherrer, P. H.: Geomagnetic Activity and Hale Sector Boundaries, *Planet Space Sci.*, 29, 167–170, 1980.

Maehara, H., Shibayama, T., Notsu, S., Notsu, Y., Nagao, T., Kusaba, S., Honda, S., Nogami, D., and Shibata, K.: Superflares on solar-type stars, *Nature. Letter*, 485, 478–481, 2012.

Ricca, R. L.: Energy, helicity and crossing number relations for complex flows, in: *Tubes, Sheets and Singularities in Fluid Dynamics*, edited by: Bajer, K. and Moffatt, H. K., 139–144, Kluwer Academic Publishers, the Netherlands, 2002.

Royal Greenwich Observatory: Sunspot and Geomagnetic-Storm Data, derived from Greenwich observations, 1874–1954, London: Her Majesty's Stationary Office, 1955.

Schrijver, C. J.: Driving major solar flares and eruptions: A review, *Adv. Space Res.*, 43, 739–755, 2009.

Silverman, S. M. and Cliver, E. W.: Low-latitude auroras: the magnetic storm of 14–15 May, 1921, *J. Atmos. Sol.-Terr., Phys.*, 63, 523–535, 2001.

- Svalgaard, L., Hannah, I. G., and Hudson, H.: Flaring solar Hale Sector Boundaries, *Astrophys. J.*, 733, 49, doi:10.1088/0004-637X/733/1/49, 2011.
- Tamm, N.: Die grossen Sonnenflecken Mitte Mai und Anfang Juni 1921, *Astron. Nachr.*, 215, 209–212, 1922.
- Title, A.: Remote Triggering of Energetic Events, in: Proceedings of TIEMS conference “Space Weather and Challenges for Modern Society”, 22–24 October 2012.
- Török, T., Berger, M. A., and Kliem, B.: The writhe of helical structures in the solar corona, *Astron. Astrophys.*, 516, 11 pp., doi:10.1051/0004-6361/200913578, 2010.
- Weaver, M., Murtagh, W., Balch, C., Biesecker, D., Combs, L., Crown, M., Dogget, K., Kunches, J., Singer, H., and Zezula, L. T. D.: NOAA Technical Memorandum OAR SEC-88, Halloween Space Weather Storms, 2004.